

## HELIUM ISOTOPE VARIATIONS IN JUAN DE FUCA RIDGE BASALTS

John E. Lupton<sup>1</sup>, David W. Graham<sup>2</sup>, John R. Delaney<sup>3</sup>, and H. Paul Johnson<sup>3</sup>

**Abstract.** We have measured  $^3\text{He}/^4\text{He}$  ratios and He and Ne concentrations on a suite of 24 basalt glasses from the neovolcanic zone of the Juan de Fuca Ridge (JdFR) from 44.6°N near the Blanco Transform up to 48.0°N on the Endeavour Segment. The helium isotope ratios exhibit a clear geographic variation, with relatively constant values of 7.8  $R_A$  along the southern JdFR increasing to a maximum of 8.8  $R_A$  at 46.9°N on the Cobb Segment, and then dropping to values of ~8.0  $R_A$  at the Cobb Offset. Ratios along the Endeavour Segment further north are somewhat higher, averaging ~8.2  $R_A$ . Basalts dredged from Axial Seamount have  $^3\text{He}/^4\text{He} = 7.9\text{-}8.4 R_A$ , indicating that the seamount does not have a geochemical or isotopic signature distinct from other portions of the JdFR. This confirms that while Axial Seamount is the locus of excess magma generation, it is devoid of any hotspot or ocean island basalt geochemical signature. For the whole sample set,  $^3\text{He}/^4\text{He}$  ratios show a negative correlation with  $^{87}\text{Sr}/^{86}\text{Sr}$ . We attribute the geographical variations in  $^3\text{He}/^4\text{He}$  to broad-scale heterogeneity in the mantle source region beneath the JdFR. Beginning at Axial Seamount and further north,  $^3\text{He}/^4\text{He}$  shows a positive correlation with  $\text{Fe}_{8,0}$ , suggesting that melting dynamics in the underlying mantle may exert some control on the helium isotope ratios along part of our survey area.

## Introduction

The discovery of  $^3\text{He}$ -enriched primordial helium in deep Pacific Ocean waters and in the glassy rinds of mid-ocean ridge pillow basalts confirmed that juvenile volatiles trapped in the Earth's interior are leaking into the oceans and atmosphere at active plate boundaries and hotspots [see Lupton, 1983, and references therein]. Helium isotope ratios, like Sr and Nd isotopes, are quite distinct for mid-ocean ridge basalts (MORBs) versus ocean island basalts (OIBs). Helium isotope variations require at least three distinct mantle components [Kurz et al., 1982a; Lupton, 1983]: the MORB component with  $^3\text{He}/^4\text{He} = 6\text{-}9 R_A$  ( $R_A$  = the atmospheric ratio of  $1.39 \times 10^{-6}$ ), a  $^3\text{He}$ -enriched mantle OIB component (10-30  $R_A$ ), and a low- $^3\text{He}$  OIB component (5-7  $R_A$ ).

Although an earlier viewpoint was that helium isotope ratios in MORBs were fairly uniform, several studies have revealed considerable  $^3\text{He}/^4\text{He}$  variation in basalts along some parts of the mid-ocean ridge system. Most of these previous studies have focussed on large-scale regional variations or on hotspot - ridge-crest interaction. The one detailed study of rare gases along a short segment of the Mid-Atlantic Ridge at 14°N [Staudacher et al., 1989] found variations of ~20% in the  $^3\text{He}/^4\text{He}$  ratio. Here we report helium isotope results for a detailed survey along ~350 km of the Juan de Fuca Ridge in the northeast Pacific. We show that the  $^3\text{He}/^4\text{He}$  ratios are related to geographic position along the JdFR axis, probably due to variations in the mantle source, and that the fine-scale structure in  $^3\text{He}/^4\text{He}$  in this region may be related to systematic changes in melting dynamics of heterogeneous upper mantle.

## Geologic Setting

The Juan de Fuca Ridge (JdFR) is a medium-rate spreading center (half rate ~3 cm/yr) located about 450 km west of the Oregon coast [Delaney et al., 1981; Johnson and Holmes, 1989]. The JdFR extends some 500 km from the Blanco Fracture Zone in the south to the Sovanco Fracture Zone in the north, and consists of several ridge segments with markedly different morphologies. Along the southernmost Cleft Segment, the ridge is marked by an axial valley and young lava flows, while north of Axial Seamount the Cobb segment is characterized by a narrow ridge axis and a shallow axial graben. At 47°40'N, the Cobb Offset separates the main portion of the JdFR from the Endeavour Segment to the north [Johnson and Holmes, 1989]. At its northern end the Cobb Segment deepens and becomes a sediment-covered graben that forms the eastern limb of the Cobb Offset. In a similar manner, the southern end of the Endeavour Segment forms the western limb of the Cobb overlayer. The Endeavour Segment is marked by a series of split ridges which progressively lengthen to the south and by an increased abundance of E-MORBs [Karsten et al., 1990]. Vigorous hydrothermal activity occurs at several localities along the JdFR axis, including several sites on the Cleft Segment, within the caldera of Axial Seamount, and on the Endeavour Segment [see Johnson and Holmes, 1989, and references therein].

One of the major topographic features of the JdFR is Axial Seamount, an active volcano which sits astride the ridge axis at latitude 46°N and stands some 800 m above the 2300-m average depth of the JdFR axis. Axial Seamount is located very near the geometric intersection of the Cobb-Eickelberg seamount chain with the ridge axis, and is thought to be the youngest volcano in this chain produced by the so-called Cobb hotspot [Delaney et al., 1981]. However, geochemical studies of JdFR basalts including samples from the summit of Axial Seamount do not support a hotspot or mantle plume origin for the volcano. Fresh, zero-age basalts are found along most of the JdFR axis and are generally Fe and Ti enriched, with higher Fe-Ti concentrations occurring in association with propagating rifts at the JdFR-Blanco Transform intersection and along the Cobb Segment near the Cobb Offset [Delaney et al., 1981]. Major elements, trace elements, and Sr isotopes exhibit measurable variation along the JdFR axis [Eaby et al., 1984; Rhodes et al., 1990; Desonie and Duncan, 1990]. However, in contrast to what would be expected for an enriched or mantle plume source, the Pb-Sr-Nd isotopic characteristics of Axial Seamount and Cobb hotspot basalts cannot be readily distinguished from the general JdFR MORB field [Eaby et al., 1984; Hegner and Tatsumoto, 1989; Desonie and Duncan, 1990]. On the other hand, Axial Seamount lavas do display subtle differences in major element chemistry relative to those on adjoining ridge segments. Thus Axial Seamount appears to be the locus of excess magma generation along the ridge axis rather than a geochemically distinct OIB-type mantle plume [Rhodes et al., 1990]. As we discuss below, while helium isotope measurements should be another sensitive indicator of a plume or hotspot component, we again find no evidence for a distinct source beneath Axial Seamount.

## Sampling and Analytical Methods

With the exception of three samples collected with the DSRV ALVIN during the 1991 NOAA/PMEL dive series on the JdFR, all of the samples for this study were acquired by dredging from surface ships during 4 different expeditions (R/V T.G Thompson, TT-152 in 1980, TT-170 in 1982, TT-175 in 1983, and cruise 81-017 of the R/V Hudson, 1981). Most of the samples used in the

<sup>1</sup>NOAA/PMEL, Newport, OR 97365<sup>2</sup>Oregon State University, Corvallis, OR 97331<sup>3</sup>University of Washington, Seattle, WA 98195

Copyright 1993 by the American Geophysical Union.

Paper number 93GL01271

0094-8534/93/93GL-01271\$03.00

present study are a subset of those analyzed by *Eaby et al.* [1984] for strontium isotopes. The three ALVIN samples are from a group of pillow mounds on the Cleft Segment which appear to have erupted between 1981 and 1987 [Chadwick et al., 1991; Embley et al., 1991].

Fresh glass chips ~1-5 mm in size were prepared and analyzed following established procedures [Graham et al., 1990]. Helium isotope ratios and He and Ne concentrations were determined on two different mass spectrometer systems: one at the Scripps Institution of Oceanography and another at U.C. Santa Barbara (UCSB). In 1991 the UCSB instrument was moved to the NOAA/PMEL facility at Newport, Oregon. As indicated by five replicate analyses of sample TT152-37-1 (Table 1), the results from the three different laboratories agree within analytical precision. In every case the gases were released from the basalt glass samples by *in vacuo* crushing. He/Ne ratios were determined to about 10% by voltage switching. The  $2\sigma$  precision for  $^3\text{He}/^4\text{He}$  determinations is about 1.2% for the SIO instrument and about 0.6% for the UCSB-NOAA spectrometer system.

### Results and Discussion

We measured helium isotope ratios on 24 distinct samples spanning the JdFR axis from latitude  $44^{\circ}37.1'N$  near the Blanco Fracture Zone up to  $48^{\circ}1.3'N$  on the Endeavour Segment. The average spacing between samples is about 30 km. Figure 1 shows the helium isotope ratios ( $R/R_A$ ) and sample locations vs. latitude. The helium isotope results are also listed in Table 1. For the purposes of this discussion, we have grouped our samples into four broad geographic regions along the JdFR: south rift (including the Cleft and Vance segments), Axial Seamount, north rift (Cobb Segment), and Endeavour Ridge.

As shown in Figure 1, there is a smooth geographical variation in the basaltic  $^3\text{He}/^4\text{He}$  ratio along the JdFR axis. Samples from the south rift have relatively uniform  $^3\text{He}/^4\text{He}$  ratios of  $7.75\text{--}7.93 R_A$ . The three ALVIN samples collected from the youngest lavas along the Cleft Segment have ratios of  $7.85 R_A$ , similar to the dredged basalts recovered along the south rift. Thus the basalts from the southern JdFR all appear to be derived from a similar mantle source, as suggested previously [Eaby et al., 1984]. The  $^3\text{He}/^4\text{He}$  ratios increase to the north as one approaches and crosses over the summit of Axial Seamount, reaching a value of  $8.36 R_A$  at the summit. However, the ratios continue to increase to the north along the northern rift or Cobb Segment, reaching a maximum of  $\sim 8.8 R_A$  at latitude  $46^{\circ}52'N$ . As the ridge begins to deepen toward the Cobb Offset the  $^3\text{He}/^4\text{He}$  ratio again decreases to values as low as  $7.9 R_A$ .

It should be emphasized that although we have observed a very clear variation of over 12% in  $^3\text{He}/^4\text{He}$  related to location along the JdFR, all of these helium isotope ratios are within the normal range of variation for MORBs. Thus it is not necessary to invoke the presence of a hotspot or OIB component in order to explain the observed variation in  $^3\text{He}/^4\text{He}$  in JdFR basalts. The strong dependence of  $^3\text{He}/^4\text{He}$  on latitude along the ridge suggests that the observed helium isotope variations reflect fundamental heterogeneities in the upper mantle beneath the ridge. Furthermore, it is clear from the results displayed in Figure 1 that Axial Seamount does not have a helium isotope signature which is distinct from other basalts along the JdFR axis. This confirms that, while Axial Seamount clearly represents the site of excess magma generation, it does not have a distinct geochemical signature.

Looking in detail at the Cobb Offset, the two samples closest to the Cobb Segment and Endeavour Segment rift tips have slightly lower  $^3\text{He}/^4\text{He}$  ratios than samples more distant from the propagating rift tip. For example, TT170-78D, which was collected just to the west of the very tip of the axial magnetic high, has a lower  $^3\text{He}/^4\text{He} = 7.9 R_A$  than other samples from the Cobb Segment which average about  $8.4\text{--}8.6 R_A$  (Fig. 1). Similarly, HU81-017-11, which is the southernmost sample from the Endeavour Segment, has a ratio of  $8.0 R_A$ , similar to that measured for TT170-78D and lower than the other Endeavour Ridge samples which have ratios of  $8.17\text{--}8.25 R_A$ . This apparent negative correlation of  $^3\text{He}/^4\text{He}$  with proximity to the Cobb propagator rift

tips suggests that the helium isotope ratios may be affected to some degree by the same processes responsible for the Fe-Ti enrichments [Christie and Sinton, 1981]. However, the fact that  $^3\text{He}/^4\text{He}$  is not well correlated with Fe-Ti enrichment along the JdFR [see Delaney et al., 1981] and that we see little change in the helium isotope ratio at JdFR intersection with the Blanco Transform where rift propagation has also occurred, indicates that rift propagation does not exert a major control on helium isotope ratios.

There are systematic variations between helium isotopes and other geochemical parameters along the JdFR which are also dependent on geographic location. Figure 2A shows that there is a good overall negative covariation of  $^3\text{He}/^4\text{He}$  with  $^{87}\text{Sr}/^{86}\text{Sr}$ . The northern rift (Cobb Segment) has slightly more depleted  $^{87}\text{Sr}/^{86}\text{Sr}$  for the samples studied here and also slightly higher  $^3\text{He}/^4\text{He}$  ratios, compared to the southern rift samples which are slightly more radiogenic in both He and Sr isotopes. This negative correlation between He and Sr isotopes is similar to that observed for large portions of the Mid-Atlantic Ridge away from the influence of high  $^3\text{He}$  hotspots [Kurz et al., 1982b; Graham et al., 1992]. The He and Sr isotope ratios for the northern rift are approaching those found in basalts from  $2\text{--}7^{\circ}S$  on the Mid-Atlantic Ridge, which collectively have the most depleted He, Sr, and Pb isotope compositions found in MORB [Graham et al., 1992].

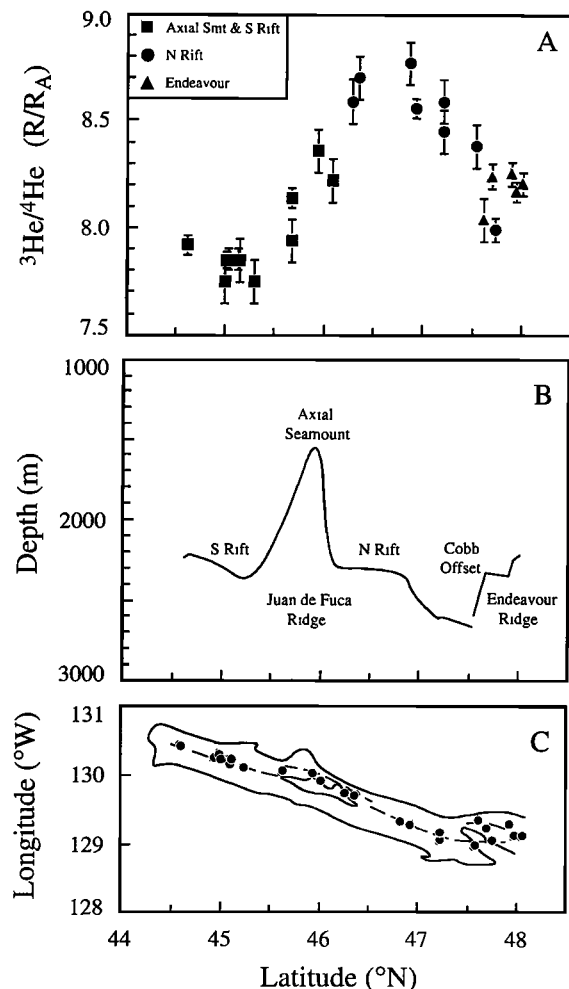


Figure 1. Helium isotope ratios, axial depth and sample locations vs. latitude along the JdFR. Helium isotope ratios are reported as  $R/R_A$ , where  $R = ^3\text{He}/^4\text{He}$  and  $R_A = 1.39 \times 10^{-6}$ , the atmospheric ratio. Error bars show  $\pm 2\sigma$  uncertainties. In panel C) the solid line indicates the  $+200\gamma$  magnetic anomaly boundary, and the dashed line traces the neovolcanic zone.

Table 1. Helium Isotopes in Juan de Fuca Ridge Basalts

Location	Sample	Latitude °N	Longitude °W	$^3\text{He}/^4\text{He}$	[He]	$\text{He}/\text{Ne}$	Lab
				R/R <sub>A</sub>	μccSTP/g	(He/Ne) <sub>air</sub>	
S Rift	TT152 37-1	44.618	130.390	7.85	15.6	>14,000	SIO
	replicate			7.91	17.1	nd	UCSB
	replicate			7.86		>15,000	UCSB
	replicate			7.92	17.7	>25,000	UCSB
	replicate			7.93	18.6	>21,000	HMSC
S Rift	TT152 43-19	44.993	130.205	7.75	1.4	>2,700	SIO
S Rift mound 1	ALV2432-1	45.017	130.217	7.85	5.8	21,000	HMSC
S Rift mound 2	ALV2432-3	45.025	130.208	7.85	0.3	650	HMSC
S Rift mound 8	ALV2430-1	45.133	130.167	7.85	2.1	6,100	HMSC
S Rift	TT152 44	45.135	130.188	7.85	2.6	>3,600	SIO
S Rift	TT152 47-39	45.295	130.087	7.75	8.0	>25,000	SIO
Axial Smt S flank	TT152 77-6	45.672	130.063	7.94	7.4	>19,000	SIO
Axial Smt S flank	TT152 77-7	45.672	130.063	8.14	8.3	12,000	HMSC
Axial Smt summit	TT152 55-25	45.938	129.993	8.36	5.7	>12,000	SIO
Axial Smt N flank	TT152 61	46.075	129.900	8.22	1.1	2,400	SIO
N Rift	TT152 72	46.278	129.730	8.59	6.1	>6,000	SIO
N Rift	TT152 65	46.353	129.678	8.70	1.3	>14,000	SIO
N Rift	TT152 29-1	46.860	129.298	8.77	6.5	>4,700	SIO
N Rift	TT152 21	46.925	129.262	8.51	11.0	>3,600	SIO
	replicate			8.56	11.6	9,800	HMSC
N Rift	TT152 13	47.208	129.120	8.59	5.2	>11,000	SIO
N Rift	HU81 017-6-11	47.210	129.082	8.45	8.5	>8,600	SIO
N Rift	TT152 11-21	47.542	128.963	8.38	0.8	960	SIO
N Rift tip	TT170 78	47.732	129.003	7.88	0.21	550	SIO
	replicate			7.99	1.5	>6,500	HMSC
Endeavour Rift tip	HU81 017-11	47.620	129.288	8.04	1.8	2,500	SIO
Endeavour	TT175 40-1	47.698	129.202	8.24	1.9	5,400	HMSC
Endeavour	TT175 36-3	47.895	129.240	8.25	2.0	nd	HMSC
Endeavour	TT175 28-24	47.947	129.103	8.17	4.6	>16,500	HMSC
Endeavour	TT175 31-2	48.022	129.067	8.21	2.1	>7,000	HMSC

SIO-Scripps Institution of Oceanography, UCSB-University of California at Santa Barbara, HMSC-Hatfield Marine Science Center

All analyses were performed by crushing *in vacuo*. 2σ uncertainties in  $^3\text{He}/^4\text{He}$  ratio, computed as the quadrature sum of in-run statistical errors plus uncertainties in air standard and blank analyses, are ±0.10 R<sub>A</sub> for SIO and ±0.05 R<sub>A</sub> for others.

There also appears to be some control on the  $^3\text{He}/^4\text{He}$  in JdFR basalts by the dynamics of melting in the underlying mantle. Figure 2B shows  $^3\text{He}/^4\text{He}$  against  $\text{Fe}_{8.0}$  for the same samples.  $\text{Fe}_{8.0}$  is calculated according to the methods of *Klein and Langmuir* [1987]. Along the south rift of the JdFR  $^3\text{He}/^4\text{He}$  ratios are constant at ~7.85 R<sub>A</sub>, and there is no covariation between  $^3\text{He}/^4\text{He}$  and  $\text{Fe}_{8.0}$ . However, to the north there is an increase in  $^3\text{He}/^4\text{He}$  with increasing  $\text{Fe}_{8.0}$ . This trend includes the Endeavour Ridge E-MORBs with lower  $^3\text{He}/^4\text{He}$  and  $\text{Fe}_{8.0}$ , and samples from the northern section of Axial Seamount. The one exception to this trend is sample TT170-78D which is from the very tip of the JdFR at the Cobb Offset. A similar, but negative correlation and with slightly more scatter is also observed between  $^3\text{He}/^4\text{He}$  and  $\text{Na}_{8.0}$  (not shown).

A positive correlation between  $^3\text{He}/^4\text{He}$  and  $\text{Fe}_{8.0}$  such as we have observed north of Axial Seamount might be expected on the basis of the simple melting column model of *Klein and Langmuir* [1987]. In this model,  $\text{Fe}_{8.0}$  may be taken as an indicator of the average depth of melting for accumulated melts. Upwelling mantle with an initial temperature above that of average mantle will intersect its solidus slightly deeper and produce melts which have a slightly higher  $\text{Fe}_{8.0}$  and lower  $\text{Na}_{8.0}$  (compared to average mantle), because it will melt over a larger depth interval and to a

somewhat larger extent. U and Th in peridotite is primarily located in clinopyroxene [*LaTourrette and Burnett*, 1992], and consequently this is where a substantial portion of upper mantle radiogenic He will be located. Clinopyroxene will contribute a relatively smaller proportion to melts formed by larger extents of non-modal melting than to melts formed by smaller extents of melting [e.g., *Kinzler and Grove*, 1992]. Assuming that JdFR basalts are the result of partial melting of upper mantle peridotite which is chemically and isotopically heterogeneous [*Zindler et al.*, 1984], then hotter mantle will melt to a larger extent and produce parental magmas which have incorporated proportionately less clinopyroxene, and thus may have lower  $\text{Na}_{8.0}$ , higher  $\text{Fe}_{8.0}$ , and slightly higher  $^3\text{He}/^4\text{He}$ .

#### Summary and Conclusions

In summary, we have observed rather large (~12%) variations in  $^3\text{He}/^4\text{He}$  ratios in basalts collected along the rift axis of the JdFR. The  $^3\text{He}/^4\text{He}$  ratios vary smoothly with location along the JdFR, are negatively correlated with  $^{87}\text{Sr}/^{86}\text{Sr}$ , and uncorrelated with Fe-Ti enrichment. For these reasons we attribute most of the observed variations in  $^3\text{He}/^4\text{He}$  to basic heterogeneity in the mantle source region beneath the ridge rather than to any shallow process

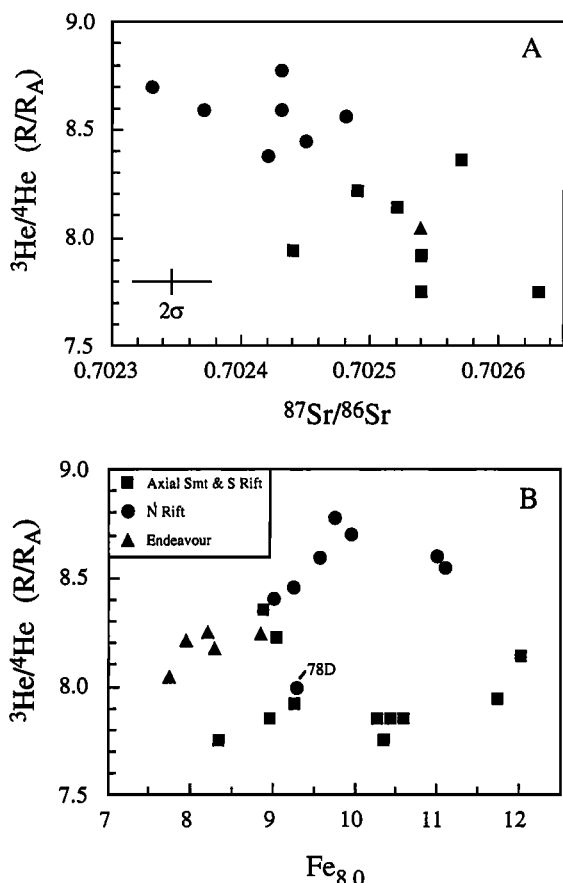


Figure 2. A)  $^3\text{He}/^4\text{He}$  vs.  $^{87}\text{Sr}/^{86}\text{Sr}$  for samples from the JdFR. Symbols are the same as Fig. 1. The crossed lines indicate  $\pm 2\sigma$  uncertainties. Strontium isotope data are from Eaby et al., [1984]. A linear least-squares fit to these data gave a linear correlation coefficient of  $r = .741$ . B)  $^3\text{He}/^4\text{He}$  vs.  $\text{Fe}_{8.0}$ . Symbols are the same as in Figure 1 and 2A.  $\text{Fe}_{8.0}$  is calculated following Klein and Langmuir [1987]. Major element data are from Eaby et al. [1984], Karsten et al. [1990], Smith et al. [1993], and Delaney [unpublished data].

involving the ridge-crest magma chamber. The lack of any distinct shift in  $^3\text{He}/^4\text{He}$  at Axial Seamount confirms that the seamount does not have an OIB geochemical signature. The fact that  $^3\text{He}/^4\text{He}$  is correlated with  $\text{Fe}_{8.0}$  for part of our sample set suggests that melting dynamics of heterogeneous mantle may play a role in controlling the helium isotope ratios in mid-ocean ridge lavas. Future detailed studies of helium isotope variations along petrologically well-characterized segments of the mid-ocean ridge system will provide additional tests of these ideas.

**Acknowledgements.** We thank H. Craig and R. Poreda for access to the SIO laboratory during the early stages of this project, J. Eaby and R. Embley for useful discussions, M. Smith and M. Perfit for cataloging of ALVIN samples and for access to their data prior to publication, and J. Karsten for a constructive review. This work was supported by the NOAA VENTS Program and by NSF Grants OCE81-09459 and OCE92-96104.

#### References

Chadwick, W.W., Jr., R.W. Embley, and C.G. Fox, Evidence for volcanic eruption on the southern Juan de Fuca Ridge between 1981 and 1987, *Nature* 350, 416-418, 1991.

- Christie, D.M., and J.M. Sinton, Evolution of abyssal lavas along propagating segments of the Galapagos Spreading Center, *Earth Planet. Sci. Lett.* 56, 321-335, 1981.
- Delaney, J.R., H.P. Johnson, and J.L. Karsten, The Juan de Fuca Ridge - hot spot - propagating rift system: New tectonic, geochemical, and magnetic data, *J. Geophys. Res.* 86, 11747-11750, 1981.
- Desonie, D. L. and R. A. Duncan, The Cobb-Eickelberg Seamount chain: hotspot volcanism with mid-ocean ridge basalt affinity, *J. Geophys. Res.* 95, 12,697-12,711, 1990.
- Eaby, J., D. Clague and J. R. Delaney, Sr isotopic variations along the Juan de Fuca Ridge, *J. Geophys. Res.* 89, 7883-7890, 1984.
- Embley, R. W., W. Chadwick, M. R. Perfit and E. T. Baker, Geology of the northern Cleft Segment, Juan de Fuca Ridge: recent lava flows, sea-floor spreading, and the formation of mega plumes, *Geology* 19, 771-775, 1991.
- Graham, D. W., J. E. Lupton, F. Albarède and M. Condomines, Extreme temporal homogeneity of helium isotopes at Piton de la Fournaise, Reunion Island, *Nature* 347, 545-548, 1990.
- Graham, D. W., W. J. Jenkins, J.-G. Schilling, G. Thompson, M. D. Kurz and S. E. Humphris, Helium isotope geochemistry of mid-ocean ridge basalts from the South Atlantic, *Earth Planet. Sci. Lett.* 110, 133-147, 1992.
- Hegner, E., and M. Tatsumoto, Pb, Sr, and Nd isotopes in seamount basalts from the Juan de Fuca Ridge and Kodiak-Bowie seamount chain, northeast Pacific, *J. Geophys. Res.* 94, 17839-17846, 1989.
- Johnson, H. P. and M. Holmes, Evolution and plate tectonics: a study of the Juan de Fuca Ridge. In: E. L. Winterer, D. L. Hussong and R. W. Decker, eds., *The Eastern Pacific Ocean and Hawaii, The Geology of North America* vol. N, Geological Society of America, Boulder, CO, pp. 73-92, 1989.
- Karsten, J. L., J. R. Delaney, J. M. Rhodes and R. A. Lias, Spatial and temporal evolution of magmatic systems beneath the Endeavour Segment, Juan de Fuca Ridge: tectonic and petrologic constraints, *J. Geophys. Res.* 95, 19,235-19,256, 1990.
- Kinzler, R. J. and T. L. Grove, Primary magmas of mid-ocean ridge basalts 1. Experiments and methods, *J. Geophys. Res.* 97, 6885-6906, 1992.
- Klein, E. M. and C. H. Langmuir, Global correlations of ocean ridge basalt chemistry with axial depth and crustal thickness, *J. Geophys. Res.* 92, 8089-8115, 1987.
- Kurz, M. D., W. J. Jenkins, and S. R. Hart, Helium isotopic systematics of oceanic islands and mantle heterogeneity, *Nature* 297, 43-47, 1982a.
- Kurz, M. D., W. J. Jenkins, J.-G. Schilling, and S. R. Hart, Helium isotopic variations in the mantle beneath the central North Atlantic Ocean, *Earth Planet. Sci. Lett.* 58, 1-14, 1982b.
- LaTourette, T.Z. and D. S. Burnett, Experimental determination of U and Th partitioning between clinopyroxene and natural and synthetic basaltic liquid, *Earth Planet. Sci. Lett.* 110, 227-244, 1992.
- Lupton, J. E., Terrestrial inert gases: isotope tracer studies and clues to primordial components in the mantle, *Ann. Rev. Earth Planet. Sci.* 11, 371-414, 1983.
- Rhodes, J. M., C. Morgan and R. A. Lias, Geochemistry of Axial Seamount lavas: magmatic relationship between the Cobb hotspot and the Juan de Fuca Ridge, *J. Geophys. Res.* 95, 12,713-12,733, 1990.
- Smith, M.C., M.R. Perfit, and I.R. Jonasson, Petrology and geochemistry of basalts from the southern Juan de Fuca Ridge: controls on the spatial and temporal evolution of MORB, *J. Geophys. Res.*, in press, 1993.
- Staudacher, T., P. Sarda, S. H. Richardson, C. J. Allègre, I. Sagna and L. V. Dmitriev, Noble gases in basalt glasses from a Mid-Atlantic topographic high at 14°N: geodynamic consequences, *Earth Planet. Sci. Lett.* 96, 119-133, 1989.
- Zindler, A., H. Staudigel and R. Batiza, Isotope and trace element geochemistry of young Pacific seamounts: implications for the scale of upper mantle heterogeneity, *Earth Planet. Sci. Lett.* 70, 175-195, 1984.

John E. Lupton, NOAA, Pacific Marine Environmental Laboratory, Hatfield Marine Science Center, Newport, OR 97365.

David W. Graham, College of Oceanic and Atmospheric Sciences, Oregon State University, Corvallis, OR 97331.

John R. Delaney and H. Paul Johnson, School of Oceanography, University of Washington, Seattle, WA 98195

(Received: March 5, 1993)

Accepted: May 7, 1993)